

Spectroscopic, Docking and MD Simulation Analysis of an Adamantane Derivative with Solvation Effects in Different Solvents

Aamal A. Al-Mutairi, Y. Shyma Mary, Y. Sheena Mary, Sreejit Soman, Hanan M. Hassan, Monirah A. Al-Alshaikh & Ali A. El-Emam

To cite this article: Aamal A. Al-Mutairi, Y. Shyma Mary, Y. Sheena Mary, Sreejit Soman, Hanan M. Hassan, Monirah A. Al-Alshaikh & Ali A. El-Emam (2022): Spectroscopic, Docking and MD Simulation Analysis of an Adamantane Derivative with Solvation Effects in Different Solvents, Polycyclic Aromatic Compounds, DOI: [10.1080/10406638.2022.2086274](https://doi.org/10.1080/10406638.2022.2086274)

To link to this article: <https://doi.org/10.1080/10406638.2022.2086274>

 View supplementary material 

 Published online: 14 Jun 2022.

 Submit your article to this journal 

 View related articles 

 View Crossmark data 



Spectroscopic, Docking and MD Simulation Analysis of an Adamantane Derivative with Solvation Effects in Different Solvents

Aamal A. Al-Mutairi^a, Y. Shyma Mary^b, Y. Sheena Mary^b, Sreejit Soman^c, Hanan M. Hassan^d, Monirah A. Al-Alshaikh^e, and Ali A. El-Emam^f

^aDepartment of Chemistry, College of Sciences, Imam Mohammad Ibn Saud Islamic University (IMSIU), Riyadh, Saudi Arabia; ^bThushara, Kollam, Kerala, India; ^cStemskills Research and Education Lab Private Limited, Faridabad, Hariyana, India; ^dDepartment of Pharmacology and Biochemistry, Faculty of Pharmacy, Delta University for Science and Technology, Gamasa City, Egypt; ^eDepartment of Chemistry, College of Sciences, King Saud University, Riyadh, Saudi Arabia; ^fDepartment of Medicinal Chemistry, Faculty of Pharmacy, Mansoura University, Mansoura, Egypt

ABSTRACT

3-(Adamantan-1-yl)-4-(4-fluorophenyl)-1-[[4-(2-methoxyphenyl)piperazin-1-yl]-methyl]-4,5-dihydro-1H-1,2,4-triazole-5-thione (AFT) was synthesized and spectroscopic investigations have been made experimentally and theoretically. The electrostatic potential maps and frontier orbital visualizations were used to comment of molecular polarity and stability in AFT. In AFT, thione group, methoxyphenyl ring, and triazole are the strongest repulsion and attractive reactive sites. The chemical descriptors in different solvents and NLO properties are predicted. For different solvents and gas phase, UV-vis theoretical spectra are being used to assess the electronic transition. Solvation free energy in water (hydration free energy) indicates good solubility of AFT in an aqueous medium, factor that corroborates the biological activity, in as much as that bioorganic processes occur in aqueous medium. Solvation produces a lowering of absorption in the UV-vis region. After evaluating the drug likeness properties, the title compound was examined for its analgesic activity by means of molecular docking and MD simulations. The MD simulations and docking studies suggested inhibitory activity against analgesic protein glutamate receptor.

ARTICLE HISTORY

Received 22 October 2021
Accepted 24 May 2022

KEYWORDS

DFT; adamantane; solvent effects; MD simulations

Introduction

Researchers are increasingly focused on developing novel and safe therapeutic molecules for medical use. Heterocyclic medicines containing nitrogen are readily accessible on the market. Triazoles are nitrogen containing molecules that serve as a major pharmacophore in a variety of biological processes.¹ Because of their intriguing structural properties and biological activity, triazoles have piqued the curiosity of many scientists in agricultural and therapeutic domains.^{2,3} The varied capabilities of triazoles and its derivatives in pharmacology, food, and agriculture have drawn a lot of attention in recent years. Numerous derivatives, for example, have been identified as agrochemicals with significant biological action.^{4,5} Anti-TB activity of triazole with diverse functional groups has been reported.^{6,7} Adamantane is a widely utilized molecular platform for

CONTACT Y. Sheena Mary  marysheena2018@rediffmail.com  Thushara, Neethinagar-64, Pattathanam, Kollam 21, Kerala, India

 Supplemental data for this article can be accessed online at <https://doi.org/10.1080/10406638.2022.2086274>.

making rigid non-aromatic ligands that are used to make thermally stable metal organic frameworks.⁸ Transition metal carbene complexes are the most common coordination compounds with azoles bearing an adamantane molecule.⁹ Alsayed et al. reported design and biological evaluation of adamantane against tuberculosis.¹⁰ Zefirov et al. reported tubulin targeted antimetabolic agents based on adamantane.¹¹ DNA cross linking agents and retinoic acid ligands are among the anticancer drugs that include the adamantane component.¹² The core structural units of physiologically active chemicals and innovative materials are functional adamantane derivatives.^{13–15}

Spectroscopic investigations and docking studies of biologically active adamantane derivatives are reported recently.^{16,17} Potential ligands for the production of metal complexes include piperazine and its derivative compounds containing other appropriate donor atoms.¹⁸ Substitution on both nitrogens of piperazine produce symmetrically di-substituted compounds as well as symmetrically mono di-substituted derivatives.¹⁹ Piperazine based ligands are unique in nature since they can be easily adjusted to fit a specific application. Piperazine and its derivatives are extremely important in biology and due to their broad spectrum of activity, they are also found in many commercial medications.^{20,21} Piperazine is the third most commonly utilized nitrogen-based pharmacophore according to the US FDA.²² Al-Alshaikh et al. reported XRD analysis of AFT.²³

Computational chemistry is now a well-known collaborator with experimental chemistry. In the recent decade, there has also been a surge interest in quantum chemical computations. Thus, theoretical calculations were done to understand how the AFT molecule interacts and frontier molecular orbitals, reactivity descriptors and molecular electrostatic potential maps were investigated for this purpose. Also, solvents effects, spectroscopic, and MD simulations are reported for AFT in the present study.

Methods

AFT is synthesized as reported²³ and vibrational (Supplementary material, Figures S1 and S2) were recorded on a DR/Jasco FT-IR and Bruker RFS instruments. Theoretical analysis were done by Gaussian09 and GaussView5 at B3LYP-D3(BJ)/6-311 + G(5D, 7F) level^{24,25} and wavenumbers are assigned by means of GAR2PED software.²⁶ The MD simulations studies were carried on the docked complexes for protein with AFT using the Desmond 2020.1 from Schrödinger, LLC. The sampling was done using same parameters for MD run in order to obtain reproducibility of the results. The OPLS-2005 force field^{27–29} and explicit solvent model with the SPC water molecules were used in this system.³⁰ Na⁺ were included for neutralizing charges. 0.15 M, NaCl solutions included in the system to simulate physiological environment. Initially, system was equilibrated using NVT ensemble for 100 ps to retrain over the protein-AFT complex. Followed by this a short run equilibration and minimization using NPT ensemble for 12 ps. The NPT ensemble was set with temperature 27 °C, the relaxation time of 1.0 ps and pressure 1 bar maintained in all the simulations.³¹ Martyna-Tuckerman-Klein chain coupling scheme³² barostat method was used for pressure control with a relaxation time of 2 ps. Particle mesh³³ was used for finding electrostatic interactions, and the radius for the coulomb interactions were fixed at 9 Å. RESPA integrator was used for 2 fs step for each trajectory to calculate the bonded forces. The RMSD, Rg, RMSF, and H-bonds were calculated to monitor the stability of the MD simulations.

Results and discussion

Geometrical parameters (DFT/XRD)

For AFT (Figure 1 and Supplementary material, Table S1), in the piperazine: C55-N8 = 1.4775/1.4683 Å, C52-N8 = 1.4694/1.4643 Å, C58-N7 = 1.4743/1.4543 Å, C49-N7 = 1.4722/1.4613 Å, C55-

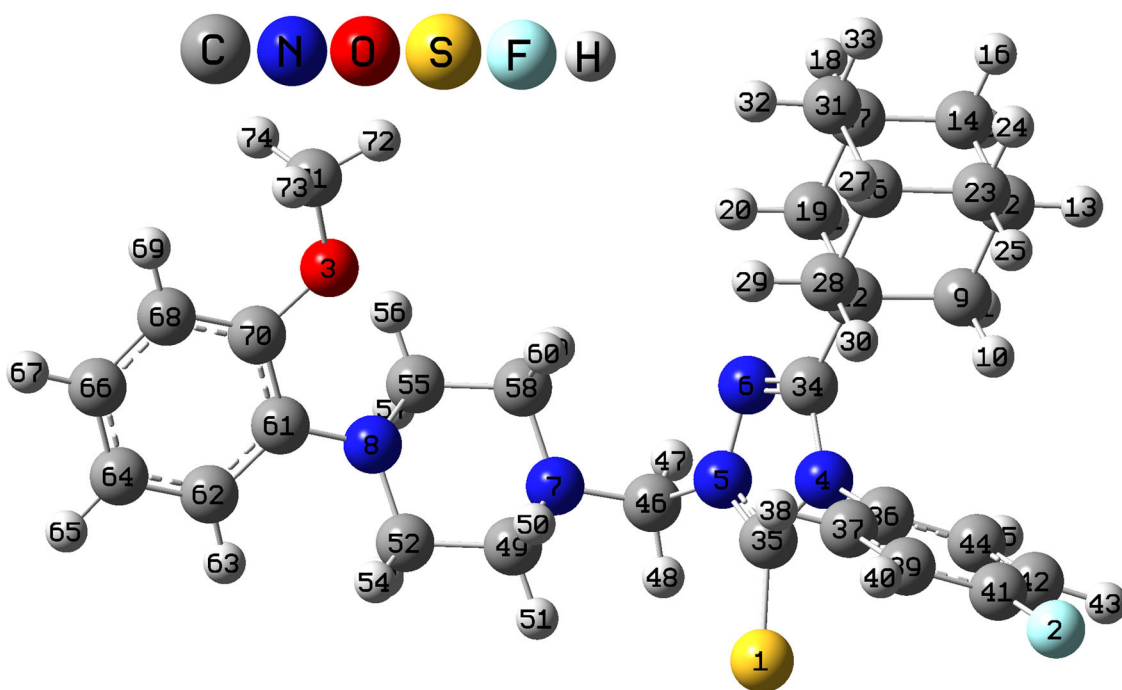


Figure 1. Optimized geometry of AFT.

C58 = 1.5269/1.5103 Å, C52-C49 = 1.5312/1.5123 Å and reported values are 1.465, 1.463, 1.458, 1.471, 1.511, 1.514 Å³⁴ and 1.488, 1.485, 1.488, 1.477, 1.547, 1.535 Å, respectively.³⁵ The adamantane CC lengths are 1.5626–1.5443/1.5424–5004 Å while reported values are 1.5422–1.5573 Å (DFT), 1.5195–1.5395 Å (XRD)³⁶ and 1.5406–1.5563 (DFT), 1.5223–1.542 (XRD).³⁷ The phenyl ring CC bond lengths are 1.4222–1.3860/1.4011–1.3674 Å (PhI) and 1.3972–1.3869/1.3773–1.3514 Å (PhIV)³⁶ and the reported values are 1.3885–1.4052 (DFT), 1.3634–1.3994 (XRD).³⁷ For AFT, lengths of CS and CF are 1.7179/1.6612 Å and 1.3896/1.3653 Å and corresponding reported values are 1.6766/1.6818 Å³⁵ and 1.3538/1.3572 Å.³⁸ For methoxy phenyl derivatives the CO lengths are 1.4391–1.3701 Å,³⁷ 1.4042, 1.4378,³⁹ and for AFT, CO lengths are 1.4012/1.3743 Å and 1.4504/1.3993 Å. In AFT pyrazole ring of AFT, CN lengths are: C34 = N6 = 1.3181/1.3093 Å, C34-N4 = 1.4080/1.3903 Å, C35-N4 = 1.4049/1.3873 Å, C35-N5 = 1.3637/1.3423 Å and reported data are, 1.3025/1.2941 Å, 1.3936/1.3722 Å, 1.3590/1.3322 Å, and 1.4017/1.3744 Å, respectively.⁴⁰ N-N length for AFT is 1.3991/1.3843 Å and reported values are 1.3693–1.3771/1.3688–1.3944 Å (DFT/XRD).⁴⁰ At C35 and C34, angles are N5-C35-S1 = 129.2/128.7°, N4-C35-S1 = 127.4/128.3°, N5-C35-N4 = 103.4/103.0°, and N4-C34-N6 = 109.5/109.7°, N4-C34-C22 = 128.2/127.1°, and N6-C34-C22 = 122.3/123.1° and this variations are due to interaction with neighbors.⁴⁰ At N4, 35-N4-C34 is decreased by 11.4/11.2° and the angle C34-N4-C36 is increased by 2.9/11.6° from 120° due to neighboring unit interactions.

IR, Raman, and VCD spectra

Vibrational experimental data with theoretical values are given in Table S2 (Supplementary material) (PhI and PhIV-ortho and para phenyl rings, PhII and PhIII –piperazine and triazole rings and PhV is the adamantane ring).

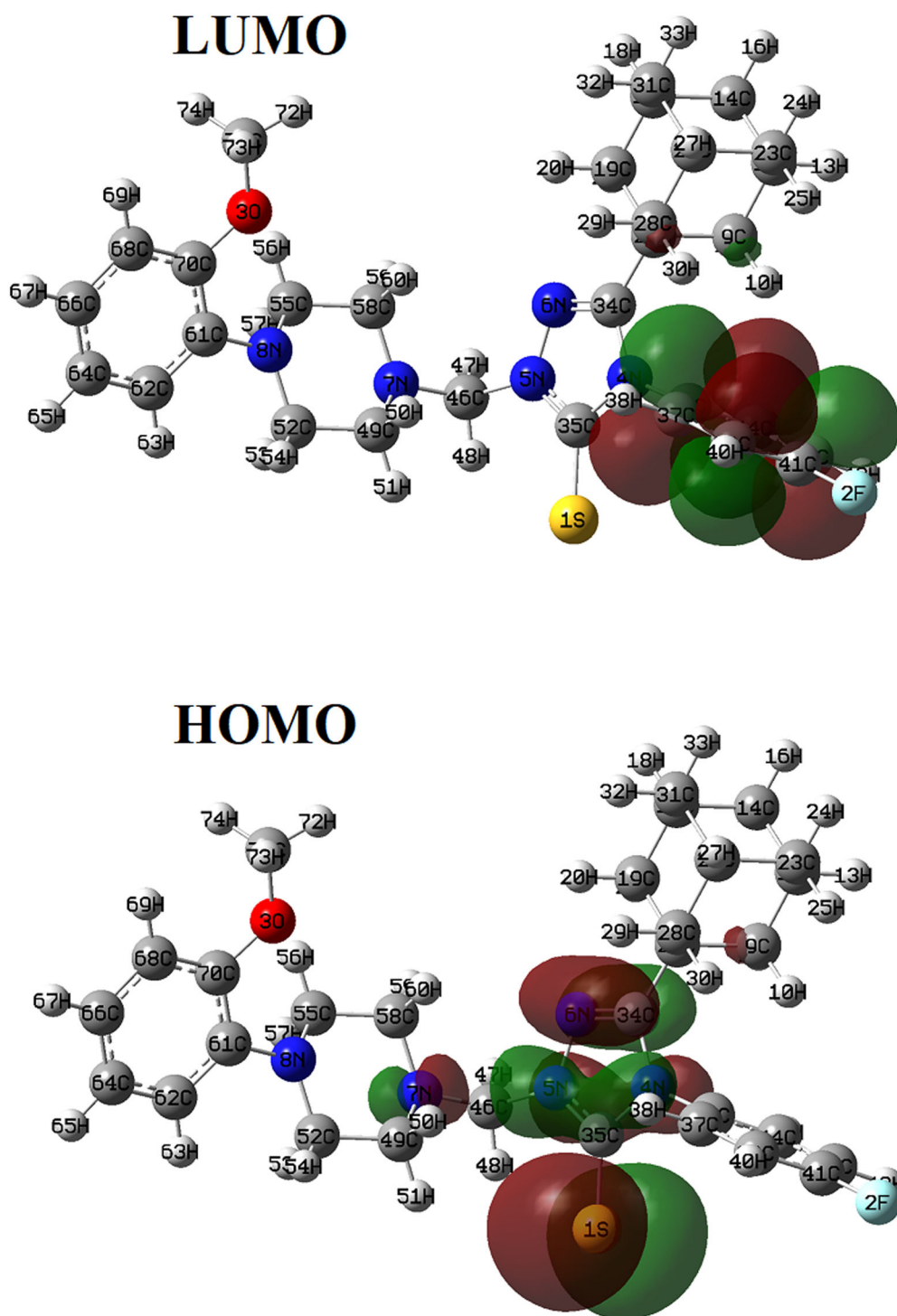


Figure 2. HOMO-LUMO plots of AFT.

Table 1. Calculated energy parameters for AFT at B3LYP-D3(BJ)/6-311 + G(5D, 7F).

Parameters	Vacuum	Benzene	Methanol	Water
Energy (au)	-2011.802400	-2011.451967	-2011.457388	-2011.437714
Solvation energy (eV)	-	-9.54	-9.39	-9.92
EHOMO (eV)	-6.9550	-6.5800	-6.7218	-6.7324
ELUMO (eV)	-0.4643	-0.3992	-0.4895	-0.4920
EHOMO-LUMO (eV)	6.4907	6.1808	6.2323	6.2404
Hardness (eV)	3.2454	3.0904	3.1162	3.1202
Chemical potential (eV)	-3.7097	-3.4896	-3.6057	-3.6122
Electrophilicity index (eV)	2.1202	1.9702	2.0860	2.0909

Adamantane ring modes

For AFT, the νCH_2 are in the region 2961–2880 and the CH_2 bending modes at 1471–868 cm^{-1} (DFT), at 1320 (IR), 1260 cm^{-1} (Raman).^{41,42} The adamantane νCC are from 668 to 1019 cm^{-1} (DFT) with bands at 781, 918 (IR) and at 783 cm^{-1} (Raman). The band at 783 cm^{-1} (DFT) and 781 cm^{-1} (IR) is identified as cage breathing mode.⁴³ Haress et al.⁴⁴ reported these C-C modes at 1003, 652, 748, 780 cm^{-1} (IR) and 658–1091 cm^{-1} (DFT) and Al-Abdullah et al.³⁶ gave these at 738, 840, 915, 952, 1025 cm^{-1} (IR), 739, 936, 953, 1023 cm^{-1} (Raman) 740–1022 cm^{-1} (DFT).

Piperazine ring modes

The piperazine νCH_2 are at 3000, 2851 cm^{-1} (IR), 3020, 2947 cm^{-1} (Raman) and at 3024 to 2811 cm^{-1} (DFT) for AFT and reported values (IR/Raman) are at 3014, 2977, 2876, 2820/2999, 2981, 2885, 2843 cm^{-1} .⁴⁵ The corresponding CH_2 deformations modes of AFT could be assigned to 1372 cm^{-1} in IR and to 1470, 1387 cm^{-1} (Raman) and from 1478 to 843 cm^{-1} (DFT).⁴⁵ Piperazine ring stretching modes in AFT is present at 907 cm^{-1} (Raman) and theoretical values are 1130, 1030, 989, 906, 895, 748 cm^{-1} .⁴⁵

Triazole ring modes

For AFT DFT analysis gives mode at 1482 cm^{-1} as $\nu\text{C}=\text{N}$ and Sebastian et al.⁴⁶ reported this mode as 1538/1540/1533 cm^{-1} in Raman/IR/DFT. The bands at 1338, 1300, 1072 cm^{-1} are the νCN modes theoretically and reported values are at 1318, 1188, 1145 cm^{-1} (IR) and at 1329, 1194, 1141 cm^{-1} (DFT)³⁵ and at 1369, 1302, 1092 cm^{-1} (DFT).⁴⁶ For AFT, νNN is at 962 cm^{-1} (DFT) with reported values at 1037⁴⁰ and at 1080 cm^{-1} .⁴⁶

Phenyl ring modes

The νCH of rings of AFT are at 3062, 3042/3075/3083, 3076, 3060, 3044 cm^{-1} (IR/Raman/DFT) for PhI and at 3105/3099, 3097, 3080, 3080 cm^{-1} (IR/DFT) for PhIV.⁴² The ring νCC are at 1572/1570, 1552, 1490, 1442, 1294 cm^{-1} (Raman/DFT) and 1572/1582, 1574, 1494, 1391, 1283/1585, 1500 cm^{-1} (Raman/DFT/IR) for PhI and PhIV, respectively.⁴² For AFT, ring breathing mode of PhI and PhIV are assigned at 1041 and at 798 cm^{-1} (DFT).^{47–51} The CH bending modes are at: 1168/1165, 1103/1283, 1168, 1101, 1034 cm^{-1} (IR/Raman/DFT) for PhI; 1009/1247, 1148, 1090, 1007 cm^{-1} (IR/DFT) for PhIV (in-plane bending) and 744/953, 909, 837, 744 cm^{-1} (IR/DFT) for PhI and 845/851/960, 937, 845, 815 cm^{-1} (IR/Raman/DFT) for PhIV (out-of-plane).⁴²

C-O, CF, CS, CH₂, and CH₂ modes

For AFT, the methoxyphenyl νCO are at 1190, 981 cm^{-1} , νCS at 516 cm^{-1} (DFT)^{41,42} and νCF is assigned at 1186 cm^{-1} .^{51,52} The νCH_3 and νCH_2 are from 3021 to 2888 and 3015 to 2956 cm^{-1} and bending modes from 1479 to 1114 and 1444 to 723 cm^{-1} (DFT).⁴²

VCD signals (Supplementary material, Figure S3) are efficient markers for identification⁵³ and ring modes show polarization at 1390 cm^{-1} (right polarization) and 1570 cm^{-1} (left polarization). The $\nu\text{CH}_2/\nu\text{CH}_3$ modes show polarization at 2968, 2951, 2903, 2819 cm^{-1} (right polarization) and 3026, 2959, 2912, 2899, 2850, 2833, 2812 cm^{-1} (left polarization). Also bending of these groups at 1305, 1257, 1174 cm^{-1} (right polarization) and at 1395, 1371, 1349, 1251, 1150 cm^{-1} (left polarization) gives polarization. The $\nu\text{C}=\text{N}$ at 1481 cm^{-1} is good marker for configuration.

Solvent effects, chemical, and electronic properties

Solvation free energies in benzene, methanol, and water were obtained through Truhlar's SMD,⁵⁴ which uses set of parameters calculated along with IEF-PCM. Solvation free energy estimates the free energy change in the transfer of a molecule between ideal gas and solvent, being important for determine different properties such as activity coefficients and solubilities.⁵⁵ For AFT, the solvation free energies were calculated via SMD model in benzene, methanol and water, which provided values equal -9.54 , -9.39 , and -9.92 eV, respectively. Although the values obtained be negative for all solvents tested, the comparison of the calculated solvation free energies values suggests that water may be better for the solubilization of AFT. However, the value of the solvation free energy in water (hydration free energy) indicates good solubility of AFT in an aqueous medium, factor that corroborates the biological activity, in as much as that bioorganic processes occur in aqueous medium.

In the present study the energies of frontier orbital were computed at DFT level and the predicted shapes of FMOs are given in Figure 2. The frontier molecular orbital energies govern molecule's stability and reactivity. The EHOMO-ELUMO gap is an important stability index of the molecules.⁵⁶ Lower the gap, softer and more polarizable is the molecule with high chemical reactivity and low kinetic stability. LUMO is over fluorophenyl ring and the HOMO is shifted mainly toward triazole and thione moieties (Figure 2). Ionization potential $I = -E_{\text{HOMO}}$ and electron affinity $A = -E_{\text{LUMO}}$. I , A , and energy gap are, 6.955, 0.4643, and 2.312 (Table 1). The chemical descriptors are: hardness $\eta = (I - A)/2$; chemical potential $\mu = -(I + A)/2$ and electrophilicity index $\omega = \mu^2/2\eta$.⁵⁷ The values of chemical descriptors are: $\eta = 3.2454$, $\mu = -3.7097$, and $\omega = 2.1202$.^{58,59}

Table 1 shows that theoretical FMOs energies and HOMO-LUMO gap calculated for AFT are somewhat lower in solution, indicating that the dielectric constant of the medium somewhat changes the reactivity of AFT, directly affecting the reactivity indexes, revealing higher values for hardness in vacuum and higher values for chemical potential in solvated media. However, in general, the calculated global reactivity descriptors compared to calculated ones for other bioactive molecules in literature⁶⁰ indicates the studied molecule as a soft molecule with good attractive electron power and moderate donating electron power.

In vacuum, the UV-vis absorptions are at 252.83 and 283.00 nm while, in solvents, only one absorption is seen, 250.88, 243.14, and 242.94 nm for benzene, methanol, and water, respectively (Supplementary material, Figure S4). Solvation produces a lowering of absorption in the UV-vis region. From the MEP plots (Figure 3) red is the strongest repulsion while blue the strongest attraction. Thione group, methoxyphenyl ring, and triazole are the strongest repulsion and attractive regions of AFT.⁶¹ The dipole moment, polarizability, first and second order hyperpolarizability are: 6.519 Debye, 5.517×10^{-23} , 4.580×10^{-30} , and -59.234×10^{-37} esu.^{37,62} The energy gap for AFT is less than urea and hyperpolarizability is 35.23 times that of urea.⁶³

The strong NBO interactions in AFT are⁶⁴: $\text{N}_4 \rightarrow \pi^*(\text{N}_6\text{-C}_{34})$, $\text{O}_3 \rightarrow \pi^*(\text{C}_{68}\text{-C}_{70})$, $\text{N}_5 \rightarrow \pi^*(\text{N}_6\text{-C}_{34})$, $\text{N}_8 \rightarrow \sigma^*(\text{C}_{61}\text{-C}_{62})$, $\text{S}_1 \rightarrow \sigma^*(\text{N}_4\text{-C}_{35})$, $\text{F}_2 \rightarrow \pi^*(\text{C}_{41}\text{-C}_{42})$ and $\text{N}_7 \rightarrow \sigma^*(\text{N}_5\text{-C}_{46})$ with the stabilization energies, 43.60, 24.96, 23.21, 21.02, 12.02, 17.00, and 17.66 kcal/mol, respectively. Almost 100% p-character is in lone pairs orbitals of S_1 , F_2 and O_3 (Supplementary material, Tables S3 and S4).

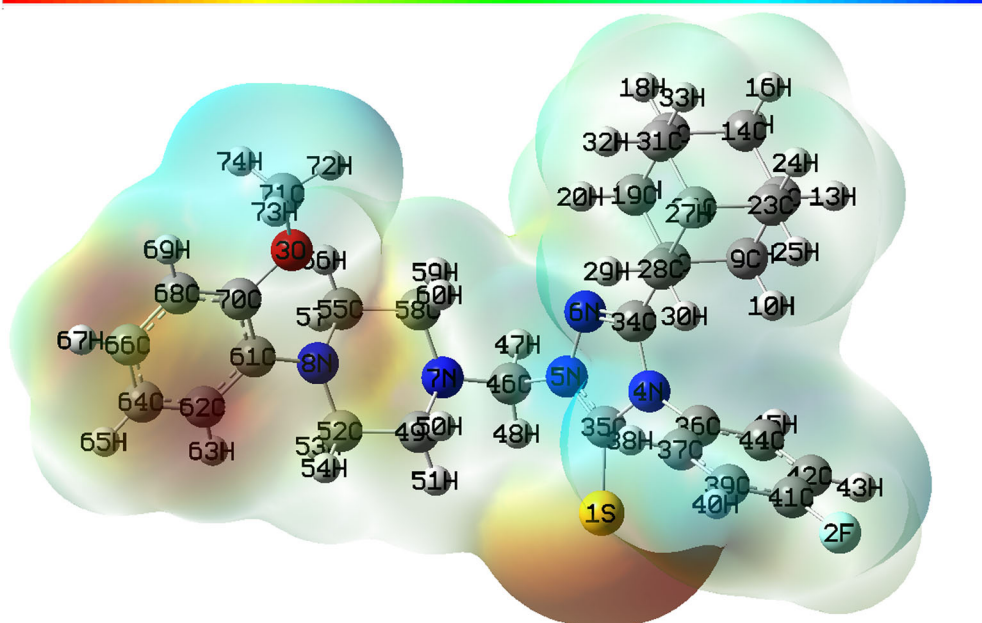
-7.544e-2**7.544e-2**

Figure 3. MEP plot of AFT.

Drug likeness and molecular dynamics simulations

To confirm the potentially active drug nature, drug similarity analysis is performed based on several pharmacophoric features of AFT, such as bioavailability, reactivity and metabolic stability. The hydrogen bond acceptors and donor's number, rotatable bonds, and molar refractivity are all essential characteristics in determining the drug similarity property of a molecule. The drug likeness test is made up of all these factors, and the values corresponding to AFT are enumerated in Table S5 (Supplementary material). Lipinski developed the Pfizer's rule of five, which consists of five rules for identifying a pharmacologically active drug.⁶⁵ The analgesic AFT had 0 and 4 hydrogen bond donors and acceptors, respectively. The number of donors should be less than 5 and the number of acceptor should be less than 10,⁶⁶ which is satisfied in the present drug analysis. Similarly for AFT, the rotatable bonds are 6 but the rule counts less than 10. The polar surface area is 70.55 \AA^2 , which is less than the allowed value of 140 \AA^2 . All of the parameters point to AFT being an active potential drug with drug qualities.

The series of adamantane derivatives in combination with carbamazepine, amantadine also produces an analgesic effect.^{67–69} PASS analysis⁷⁰ predicts analgesic activity for AFT (Supplementary material, Table S6) and hence the analgesic protein glutamate receptor (4MF3) was used for docking.^{71,72} The binding affinity is -9.5 kcal/mol (Supplementary material, Table S7) and amino acids Glu14, Asp175, Ser174, Tyr197 Glu15 forms interactions with AFT (Supplementary material, Figure S5) means AFT shows activity against glutamate receptor and can be used a new analgesic drug.

Molecular dynamics and simulation (MD) of the ligand (AFT) bound main 4MF3 was studied in details to understand the nature of possible binding motifs and structurally stable conformations. In order to obtain the information of accurate structural convergence in MD studies, replication of the simulations was done using same system parameters. The RMSD of 100 ns simulation trajectories displayed a stable conformation of the ligand bound protein (Figure 4a, red) complex with 0.2 \AA deviations. While the ligand RMSD also displayed very less deviation

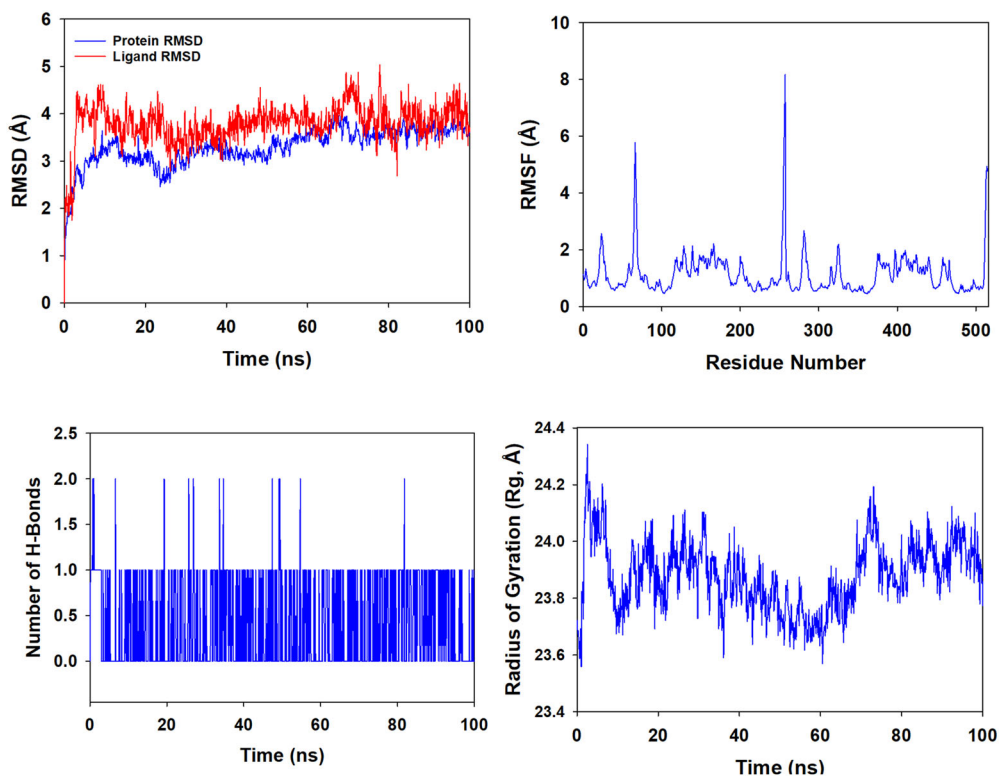


Figure 4. (a) RMSD of backbone atoms of apo and its complex with ligand, (b) Ligand RMSF of ligand complex, (c) H-bond of complex with ligand, and (d) Rg of ligand.

indicating the stable complex with 4MF3. Root mean square fluctuations of the whole C-alpha atom of 4MF3 at a function of 100 ns time scale displayed very less deviations except at 257 residue position (8 Å) indicating very stable and compact protein ligand complex (Figure 4b).⁷³

The number of Hydrogen bonds (Figure 4c) formed throughout the simulations was found to be 2. Radius of Gyration (Figure 4d) of C-alpha atom of 4MF3 displayed the conformational convergence toward a compact structure leading to a stable 4MF3- AFT complex which is also in agreement with RMSF values. The binding SASA (Figure 5a) displayed lowering of surface area in the ligand bound protein complex as compared to the unbound protein structure. This indicates the compactness of the ligand bound protein complex and suggesting an equilibrated as well as converged structure. Since the process was done for 100 ns and both shows a steady SASA values from 60 ns to 100 ns around 660 to 805 (Å²) for unbound and 165 to 280 (Å²) for the bound structures.⁷⁴

The total energy (Figure 5b) of whole system is found to be very stable and minimized global energy. The two major non bonded interactions played important role in stabilizing the complex such as van der Waals & Coulomb Energy. The Coulomb Energy displayed high contribution to achieve a global minima structure of the whole protein-ligand complex throughout the simulation time of 100 ns as compared to van der Waals energy. The screenshot of the trajectories of every 20 ns displayed very less conformational change of the ligand bound at the binding cavity of 4MF3 (Supplementary material, Figure S6). Non significant variations of the poses of every 20 ns frame were observed during the entire simulation process.^{75,76} Therefore it can be suggested that the ligand bound to the protein making a stable conformation throughout the simulation time.

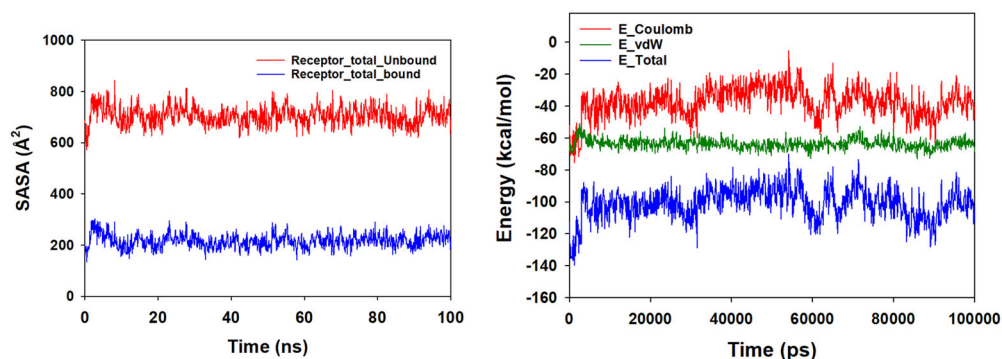


Figure 5. (a) SASA of unbound and bound receptor and (b) Energy profile of ligand complex.

Conclusion

The vibrational spectroscopic properties of AFT have been studied and vibrational assignments are done using PED. All the geometrical parameters given by DFT computations correlate with the experimental observations. The adamantane cage ring breathing mode is assigned at 783 cm^{-1} theoretically which is supported by the IR band at 781 cm^{-1} . Reactive sites, FMOs and various electronic and chemical properties in different solvents are identified. UV-vis spectra for various solvents will disclose electronic properties. The drug likeness analysis is performed to verify the drug nature of the title compound based on its bioavailability. Molecular docking supports the results of chosen the analgesic based on ligand-protein interactions. Root mean square fluctuations of the whole C-alpha atom of 4MF3 at a function of 100 ns time scale displayed very less deviations except at 257 residue position (8 \AA) indicating very stable and compact protein ligand complex. Total RMSD finding indicates that AFT binding to protein's active site is steady. Docking of AFT has binding affinities and possibly useful as a new analgesic drug agents.

Disclosure statement

The authors declare no competing interests.

Author's contributions

Conceptualization, Methodology, Writing original draft, Writing-review and editing: Aamal A. Al-Mutairi, Y. Shyma Mary, Y. Sheena Mary, Sreejit Soman, Hanan M. Hassan, Monirah A. Al-Shaikh, Ali A. El-Emam.

References

1. R. Sathyanarayana and B. Poojary, "Exploring Recent Developments on 1,2,4-Triazole: Synthesis and Biological Applications," *Journal of the Chinese Chemical Society* 67, no. 4 (2020): 459–77. doi:10.1002/jccs.201900304.
2. C. Li, J. C. Liu, Y. R. Li, C. Gou, M. L. Zhang, H. Y. Liu, X. Z. Li, C. J. Zheng, and H. R. Piao, "Synthesis and Antimicrobial Evaluation of 5-Aryl-1,2,4-Triazole-3-Thione Derivatives Containing a Rhodanine Moiety," *Bioorganic & Medicinal Chemistry Letters* 25, no. 15 (2015): 3052–6. 10.1016/j.bmcl.2015.04.081
3. B. Kahveci, E. Mentese, E. Akkaya, F. Yilmaz, İ. S. Doğan, and A. Özel, "Synthesis of Some Novel 1,2,4-Triazol-3-One Derivatives Bearing the Salicyl Moiety and Their Anticonvulsant Activities," *Archiv der Pharmazie* 347, no. 6 (2014): 449–55. doi:10.1002/ardp.201300427.
4. J. Lin, J. Lin, S. Zhou, J. X. Xu, G. F. Hao, and Y. T. Li, "Design, Synthesis, and Structure-Activity Relationship of Economical Triazole Sulfonamide Aryl Derivatives with High Fungicidal Activity," *Journal of Agricultural and Food Chemistry* 68, no. 25 (2020): 6792–801. 10.1021/acs.jafc.9b07887

5. S. Akin, E. A. Demir, A. Colak, Y. Kolcuoglu, N. Yildirim, and O. Bekircan, "Synthesis, Biological Activities and Molecular Docking Studies of Novel 2,4,5-Trisubstituted-1,2,4-Triazoles-3-One Derivatives as Potent Tyrosinase Inhibitors," *Journal of Molecular Structure* 1175 (2019): 280–6. doi:10.1016/j.molstruc.2018.07.065.
6. K. N. Venugopala, M. Kandeel, M. Pillay, P. K. Deb, H. H. Abdallah, M. F. Mahomoodally, and D. Chopra, "Anti-Tubercular Properties of 4-Amino-5-(4-Fluoro-3-Phenoxyphenyl)-4H-1,2,4-Triazole-3-Thiol and Its Schiff Bases: Computational Input and Molecular Dynamics," *Antibiotics* 9, no. 9 (2020): 559. doi:10.3390/antibiotics9090559.
7. Z. Peng, G. Wang, Q. H. Zeng, Y. Li, Y. Wu, H. Liu, J. J. Wang, and Y. Zhao, "Synthesis, Antioxidant and Anti-Tyrosinase Activity of 1,2,4-Triazole Hydrazones as Antibrowning Agents," *Food Chemistry* 341, no. Pt 2 (2021): 128265. doi:10.1016/j.foodchem.2020.128265
8. M. A. Khanfar, A. M. Jaber, M. A. AlDamen, and R. A. Al-Qawasmeh, "Synthesis, Characterization, Crystal Structure and DFT Study of New Square Planar Cu(II) Complex Containing Bulky Adamantane Ligand," *Molecules* 23, no. 3 (2018): 701. doi:10.3390/molecules23030701.
9. D. I. Pavlov, T. S. Sukhikh, and A. S. Potapov, "Synthesis of Azolyol-Substituted Adamantane Derivatives and Their Coordination Compounds," *Russian Chemical Bulletin* 69, no. 10 (2020): 1953–64. doi:10.1007/s11172-020-2985-2.
10. S. S. R. Alsayed, S. Lun, A. Payne, W. R. Bishai, and H. Gunosewoyo, "Design, Synthesis and Antimycobacterial Evaluation of Novel Adamantane and Adamantanol Analogues Effective Against Drug-Resistant Tuberculosis," *Bioorganic Chemistry* 106 (2021): 104486. doi:10.1016/j.bioorg.2020.104486
11. N. A. Zefirov, Y. A. Evteeva, A. I. Krasnoperova, A. V. Mamaeva, E. R. Milaeva, S. A. Kuznetsov, and O. N. Zefirova, "Tubulin Targeted Antimitotic Agents Based on Adamantane Lead Compound: Synthesis, SAR and Molecular Modeling," *Mendeleev Communications* 30, no. 4 (2020): 421–3. doi:10.1016/j.mencom.2020.07.005.
12. L. Wanka, K. Iqbal, and P. R. Schreiner, "The Lipophilic Bullet Hits the Targets: Medicinal Chemistry of Adamantane Derivatives," *Chemical Reviews* 113, no. 5 (2013): 3516–604. doi:10.1021/cr100264t
13. A. Schoedel and S. Rajeh, "Why Design Matters: From Decorated Metal Oxide Clusters to Functional Metal-Organic Frameworks," *Topics in Current Chemistry* 378 (2020): 19. doi:10.1007/s41061-020-0281-0.
14. Y. N. Klimochkin, E. A. Ivleva, and I. K. Moiseev, "Selective Nitroxylation of Adamantane Derivatives in the System Nitric Acid-Acetic Anhydride," *Russian Journal of Organic Chemistry* 56, no. 9 (2020): 1532–9. doi:10.1134/S10700428020090055.
15. E. V. Suslov, E. S. Mozhaytsev, D. V. Korchagina, N. I. Bormotov, O. I. Yarovaya, K. P. Volcho, O. A. Serova, A. P. Agafonov, R. A. Maksyutov, L. N. Shishkina, et al, "New Chemical Agents Based on Adamantane-Monoterpene Conjugates Against Orthopoxvirus Infections," *RSC Medicinal Chemistry* 11, no. 10 (2020): 1185–95. doi:10.1039/d0md00108b
16. L. H. Al-Wahaibi, Y. Sert, F. Uzun, N. H. Al-Shaalan, A. Alsouk, A. A. El-Emam, and M. Karakaya, "Theoretical and Experimental Spectroscopic Studies, XPS Analysis, Dimer Interaction Energies and Molecular Docking Study of 5-(Adamantan-1-yl)-N-Methyl-1,3,4-Thiadiazol-2-Amine," *Journal of Physics and Chemistry of Solids* 135 (2019): 109091. doi:10.1016/j.jpcs.2019.109091.
17. K. Karrouchi, S. A. Brandan, Y. Sert, H. El-Marzouqi, S. Radi, M. Ferbinteanu, M. E. A. Faouzi, Y. Garcia, and M. Ansar, "Synthesis, X-Ray Structure, Vibrational Spectroscopy, DFT, Biological Evaluation and Molecular Docking Studies of (E)-N'-(4-(Dimethylamino)Benzylidene)-5-Methyl-1H-Pyrazole-3-Carbohydrazide," *Journal of Molecular Structure* 1219 (2020): 128541. doi:10.1016/j.molstruc.2020.128541.
18. R. Kant, T. Kaur, Z. Hilal, N. Aggarwal, and S. Maji, "Synthesis and Characterization of a Series of Phenyl Piperazine Based Ligands," *Journal of Physics: Conference Series* 1531, no. 1 (2020): 012106. doi:10.1088/1742-6595/1531/1/012106.
19. R. Kant and S. Maji, "Recent Advances in the Synthesis of Piperazine Based Ligands and Metal Complexes and Their Applications," *Dalton Transactions* 50, no. 3 (2021): 785–800. doi:10.1039/D0DT03569F
20. C. K. Arnatt, J. L. Adams, Z. Zhang, K. M. Haney, G. Li, and Y. Zhang, "Design, Syntheses, and Characterization of Piperazine Based Chemokine Receptor CCR5 Antagonists as Anti Prostate Cancer Agents," *Bioorganic & Medicinal Chemistry Letters* 24, no. 10 (2014): 2319–23. doi:10.1016/j.bmcl.2014.03.073
21. M. Baran, E. Kepczyńska, M. Zylewski, A. Siwek, M. Bednarski, and M. T. Cegła, "Studies on Novel Pyridine and 2-Pyridone Derivatives of N-Arylpiperazine as α -Adrenoceptor Ligands," *Medicinal Chemistry (Sharīqah (United Arab Emirates))* 10, no. 2 (2014): 144–53. doi:10.2174/0929867320999131122114922
22. R. Vardanyan, *Piperidine Based Drug Discovery* (Elsevier, 2017).
23. M. A. Al-Alshaikh, A. A. Al-Mutairi, H. A. Ghabbour, A. A. El-Emam, M. S. M. Abdelbaky, and S. Garcia-Granda, "Syntheses and Crystal Structures of Two Adamantyl-Substituted 1,2,4-Triazole-5-Thione N-Mannich Bases," *Acta Crystallographica. Section E, Crystallographic Communications* 73, no. Pt 8 (2017): 1135–9. doi:10.1107/S2056989017009756

24. M. J. Frisch, G. W. Trucks, H. B. Schlegel, G. E. Scuseria, M. A. Robb, J. R. Cheeseman, G. Scalmani, V. Barone, B. Mennucci, G. A. Petersson, H. Nakatsuji, et al., *Gaussian 09, Revision B.01* (Wallingford, CT: Gaussian, Inc., 2010).
25. R. Dennington, T. Keith, and J. Millam, *Gaussview, Version 5* (Shawnee Mission, KS: Semichem Inc., 2009).
26. J. M. L. Martin and C. Van Alsenoy, *GAR2PED, a Program to Obtain a Potential Energy Distribution from a Gaussian Archive Record* (Belgium: University of Antwerp, 2007).
27. K. J. Bowers, D. E. Chow, H. Xu, R. O. Dror, B. A. Gregersen, J. L. Klepeis, I. Kolossvary, M. A. Moraes, F. D. Sacerdoti, and J. K. Salmon, "Scalable Algorithms for Molecular Dynamics Simulations on Commodity Clusters," InSc'06: Proceedings of the 2006 ACM/IEEE Conference on Supercomputing, 2006 Nov. 11, p 43. IEEE.
28. E. Chow, C. A. Rendleman, K. J. Bowers, R. O. Dror, D. H. Hughes, J. Gullingsrud, F. D. Sacerdoti, and D. E. Shaw, "Desmond Performance on a Cluster of Multicore Processors," DE Shaw Research Technical Report DESRES/TR-2008-01.
29. D. Shivakumar, J. Williams, Y. Wu, W. Damm, J. Shelley, and E. Sherman, "Prediction of Absolute Solvation Free Energies Using Molecular Dynamics Free Energy Perturbation and the OPLS Force Field," *Journal of Chemical Theory and Computation* 6, no. 5 (2010): 1509–19. [10.1021/ct900587b](https://doi.org/10.1021/ct900587b)
30. W. L. Jorgensen, J. Chandrasekhar, J. D. Madura, R. W. Impey, and M. L. Klein, "Comparison of Simple Potential Functions for Simulating Liquid Water," *The Journal of Chemical Physics* 79, no. 2 (1983): 926–35. doi:[10.1063/1.445869](https://doi.org/10.1063/1.445869).
31. G. J. Martyna, D. J. Tobias, and M. L. Klein, "Constant Pressure Molecular Dynamics Algorithms," *Journal of Chemical Physics* 101, no. 5 (1994): 4177–89. doi:[10.1063/1.467468](https://doi.org/10.1063/1.467468).
32. G. J. Martyna, M. L. Klein, and M. Tuckerman, "Nose-Hoover Chains-the Canonical Ensemble via Continuous Dynamics," *Journal of Chemical Physics* 97, no. 4 (1992): 2635–43. doi:[10.1063/1.463940](https://doi.org/10.1063/1.463940).
33. Y. A. Toukmaji and J. Board, "Ewald Summation Techniques in Perspective: A Survey," *Computer Physics Communications* 95, no. 2-3 (1996): 73–92. doi:[10.1016/0010-4655\(96\)00016-1](https://doi.org/10.1016/0010-4655(96)00016-1).
34. A. A. El-Emam, A. S. Al-Tamimi, K. A. Al-Rashood, H. N. Misra, V. Narayan, O. Prasad, and L. Sinha, "Structural and Spectroscopic Characterization of a Novel Potential Chemotherapeutic Agent 3-(1-Adamantyl)-1-[[4-(2-Methoxyphenyl)Piperazin-1-yl]-4-Methyl-1H-1,2,4-Triazole-5(4H)-Thione by First Principle Calculations," *Journal of Molecular Structure* 1022 (2012): 49–60. doi:[10.1016/j.molstruc.2012.04.074](https://doi.org/10.1016/j.molstruc.2012.04.074).
35. K. S. Resmi, Y. S. Mary, H. T. Varghese, C. Y. Panicker, M. Pakosińska-Parys, and C. V. Alsenoy, "Spectral Investigations, DFT Computations and Molecular Docking Studies of 1,7,8,9-Tetrachloro-10,10-Dimethoxy-4-{3-[4-(2-Methylphenyl)Piperazin-1-yl]Propyl}-4-Azatricyclo[5.2.1.0^{2,6}]Dec-8-Ene-3,5-Dione," *Journal of Molecular Structure* 1098 (2015): 130–45. doi:[10.1016/j.molstruc.2015.05.047](https://doi.org/10.1016/j.molstruc.2015.05.047).
36. E. S. Al-Abdullah, S. H. R. Sebastian, R. I. Al-Wabli, A. A. El-Emam, C. Y. Panicker, and C. Van Alsenoy, "Vibrational Spectroscopic Studies (FT-IR, FT-Raman) and Quantum Chemical Calculations on 5-(Adamantan-1-yl)-3-[(4-Fluoroanilino)Methyl]-2,3-Dihydro-1,3,4-Oxadiazole-2-Thione, a Potential Chemotherapeutic Agent," *Spectrochimica Acta. Part A, Molecular and Biomolecular Spectroscopy* 133 (2014): 605–18. [10.1016/j.saa.2014.06.035](https://doi.org/10.1016/j.saa.2014.06.035)
37. F. A. M. Al-Omary, Y. S. Mary, C. Y. Panicker, A. A. El-Emam, I. A. Al-Swaidan, A. A. Al-Saadi, and C. Van Alsenoy, "Spectroscopic Investigations, NBO, HOMO-LUMO, NLO Analysis and Molecular Docking of 5-(Adamantan-1-yl)-3-Anilinomethyl-2,3-Dihydro-1,3,4-Oxadiazole-2-Thione, a Potential Bioactive Agent," *Journal of Molecular Structure* 1096 (2015): 1–14. doi:[10.1016/j.molstruc.2015.03.049](https://doi.org/10.1016/j.molstruc.2015.03.049).
38. Y. S. Mary, C. Y. Panicker, M. Sapnakumari, B. Narayana, B. K. Sarojini, A. A. Al-Saadi, C. Van Alsenoy, and J. A. War, "FT-IR, NBO, HOMO-LUMO, MEP Analysis and Molecular Docking Study of 1-[3-(4-Fluorophenyl)-5-Phenyl-4,5-Dihydro-1H-Pyrazol-1-yl]Ethanone," *Spectrochimica Acta* 136 (2015): 483–93. doi:[10.1016/j.saa.2014.09.061](https://doi.org/10.1016/j.saa.2014.09.061).
39. E. S. Al-Abdullah, Y. S. Mary, C. Y. Panicker, N. R. El-Brollosy, A. A. El-Emam, C. Van Alsenoy, and A. A. Al-Saadi, "Theoretical Investigations on the Molecular Structure, Vibrational Spectra, HOMO-LUMO Analyses and NBO Study of 1-[(Cyclopropylmethoxy)methyl]-5-Ethyl-6-(4-Methylbenzyl)-1,2,3,4-Tetrahydropyrimidine-2,4-Dione," *Spectrochimica Acta. Part A, Molecular and Biomolecular Spectroscopy* 133 (2014): 639–50. [10.1016/j.saa.2014.06.042](https://doi.org/10.1016/j.saa.2014.06.042)
40. C. Y. Panicker, H. T. Varghese, P. S. Manjula, B. K. Sarojini, B. Narayana, J. A. War, S. K. Srivastava, C. Van Alsenoy, and A. A. Al-Saadi, "FT-IR, HOMO-LUMO, NBO, MEP Analysis and Molecular Docking Study of 3-Methyl-4-{(E)-[4-(Methylsulfanyl)-Benzylidene]Amino}1H-1,2,4-Triazole-5(4H)-Thione," *Spectrochimica Acta* 151 (2015): 198–207. doi:[10.1016/j.saa.2015.06.076](https://doi.org/10.1016/j.saa.2015.06.076).
41. A. S. El-Azab, Y. S. Mary, C. Y. Panicker, A. A. M. Abdel-Aziz, M. A. El-Sherbeny, and C. Van Alsenoy, "DFT and Experimental (FT-IR and FT-Raman) Investigation of Vibrational Spectroscopy and Molecular Docking Studies of 2-(4-Oxo-3-Phenethyl-3,4-Dihydroquinazolin-2-Ylthio)-N-(3,4,5-

- Trimethoxyphenyl)Acetamide,” *Journal of Molecular Structure* 1113 (2016): 133–45. doi:10.1016/j.molstruc.2016.02.038.
42. N. P. G. Roeges, *A Guide to the Complete Interpretation of Infrared Spectra of Organic Structures* (New York: John Wiley and Sons Inc., 1994).
43. L. Bisticric, L. Pejov, and G. Baranovic, “A Density Functional Theory Analysis of Raman and IR Spectra of 2-Adamantanone,” *Journal of Molecular Structure: THEOCHEM* 594, no. 1-2 (2002): 79–88. doi:10.1016/S0166-1280(02)00367-6.
44. N. G. Haress, F. A. M. Al-Omary, A. A. El-Emam, Y. S. Mary, C. Y. Panicker, A. A. Al-Saadi, J. A. War, and C. Van Alsenoy, “Spectroscopic Investigation (FT-IR and FT-Raman), Vibrational Assignments, HOMO-LUMO Analysis and Molecular Docking Study of 2-(Adamantan-1-yl)-5-(4-Nitrophenyl)-1,3,4-Oxadiazole,” *Spectrochimica Acta. Part A, Molecular and Biomolecular Spectroscopy* 135 (2015): 973–83. doi:10.1016/j.saa.2014.07.077
45. A. T. Onawole, A. F. Al-Ahmadi, Y. S. Mary, C. Y. Panicker, N. Ullah, S. Armakovic, S. J. Armakovic, C. Van Alsenoy, and A. A. Al-Saadi, “Conformational, Vibrational and DFT Studies of a Newly Synthesized Arylpiperazine Based Drug and Evaluation of Its Reactivity towards the Human GABA Receptor,” *Journal of Molecular Structure* 1147 (2017): 266–80. doi:10.1016/j.molstruc.2017.06.107.
46. S. H. R. Sebastian, M. I. Attia, M. S. Almutairi, A. A. El-Emam, C. Y. Panicker, and C. Van Alsenoy, “FT-IR, FT-Raman, Molecular Structure, First Order Hyperpolarizability, HOMO and LUMO Analysis, MEP and NBO Analysis of 3-(Adamantan-1-yl)-4-(Prop-2-en-1-yl)-1H-1,2,4-Triazole-5(4H)-Thione, a Potential Bioactive Agent,” *Spectrochimica Acta. Part A, Molecular and Biomolecular Spectroscopy* 132 (2014): 295–304. doi:10.1016/j.saa.2014.04.177
47. A. S. Devi, V. V. Aswathy, Y. S. Mary, C. Y. Panicker, S. Armakovic, S. J. Armakovic, R. Ravindran, and C. Van Alsenoy, “Synthesis, XRD Single Crystal Structure Analysis, Vibrational Spectral Analysis, Molecular Dynamics, and Molecular Docking Studies of 2-(3-Methoxy-4-Hydroxyphenyl) Benzothiazole,” *Journal of Molecular Structure* 1148 (2017): 282–92. doi:10.1016/j.molstruc.2017.07.065.
48. G. Varsanyi, *Assignments of Vibrational Spectra of Seven Hundred Benzene Derivatives* (New York: Wiley, 1974).
49. Y. S. Mary, C. Y. Panicker, B. Narayana, S. Samshuddin, B. K. Sarojini, and C. Van Alsenoy, “FT-IR, Molecular Structure, HOMO-LUMO, MEP, NBO Analysis and First Order Hyperpolarizability of Methyl 4,4'-Difluoro-5'-Methoxy-1,1':3',1''-Terphenyl-4'-Carboxylate,” *Spectrochimica Acta* 133 (2014): 480–8. doi:10.1016/j.saa.2014.06.031.
50. K. Jalaja, M. A. Al-Alshaikh, Y. S. Mary, C. Y. Panicker, A. A. El-Emam, O. Temiz-Arpaci, and C. Van Alsenoy, “Vibrational Spectroscopic Investigations and Molecular Docking Studies of Biologically Active 2-[4-(4-Phenylbutanamido)Phenyl]-5-Ethylsulphonyl-Benzoxazole,” *Journal of Molecular Structure* 1148 (2017): 119–33. doi:10.1016/j.molstruc.2017.07.023.
51. Y. Sheena Mary, K. Raju, T. E. Bolelli, I. Yildiz, H. I. S. Nogueira, C. M. Granadeiro, and C. V. Alseony, “FT-IR, FT-Raman, Surface Enhanced Raman Scattering and Computational Study of 2-(p-Fluorobenzyl)-6-Nitrobenzoxazole,” *Journal of Molecular Structure* 1012 (2012): 22–30. doi:10.1016/j.molstruc.2011.12.042.
52. N. B. Colthup, L. H. Daly, and S. E. Wiberly, *Introduction of Infrared and Raman Spectroscopy* (New York: Academic Press, 1975).
53. A. S. Al-Tamimi, Y. S. Mary, H. M. Hassan, K. S. Resmi, A. A. El-Emam, B. Narayana, and B. K. Sarojini, “Study on the Structure, Vibrational Analysis and Molecular Docking of Fluorophenyl Derivatives Using FT-IR and Density Functional Theory Computations,” *Journal of Molecular Structure* 1164 (2018): 172–9. doi:10.1016/j.molstruc.2018.03.070.
54. A. V. Marenich, C. J. Cramer, and D. G. Truhlar, “Universal Solvation Model Based on Solute Electron Density and on a Continuum Model of the Solvent Defined by the Bulk Dielectric Constant and Atomic Surface Tensions,” *The Journal of Physical Chemistry. B* 113, no. 18 (2009): 6378–96. <https://doi.org/10.1021/jp810292n>
55. G. D. R. Matos, D. Y. Kyu, H. H. Loeffler, J. D. Chodera, M. R. Shirts, and D. L. Mobley, “Approaches for Calculating Solvation Free Energies and Enthalpies Demonstrated with an Update of the FreeSolv Database,” *Journal of Chemical and Engineering Data* 62, no. 5 (2017): 1559–69. doi:10.1021/acs.jced.7b00104
56. T. K. Kuruvilla, J. C. Prasana, S. Muthu, J. George, and S. A. Mathew, “Quantum Mechanical and Spectroscopic (FT-IR, FT-Raman) Study, NBO Analysis, HOMO-LUMO, First Order Hyperpolarizability and Molecular Docking Study of Methyl[(3R)-3-(2-Methylphenoxy)-3-Phenylpropyl]Amine by Density Functional Method,” *Spectrochimica Acta* 188 (2018): 382–93. doi:10.1016/j.saa.2017.07.029.
57. R. G. Parr and R. G. Pearson, “Absolute Hardness: Companion Parameter to Absolute Electronegativity,” *Journal of the American Chemical Society* 105, no. 26 (1983): 7512–6. doi:10.1021/ja00364a005.
58. B. Sureshkumar, Y. S. Mary, C. Y. Panicker, K. S. Resmi, S. Suma, S. Armakovic, S. J. Armakovic, and C. Van Alsenoy, “Spectroscopic Analysis of 8-Hydroxyquinoline-5-Sulphonic Acid and Investigation of Its

- Reactive Properties by DFT and Molecular Dynamics Simulations,” *Journal of Molecular Structure* 1150 (2017): 540–52. doi:10.1016/j.molstruc.2017.09.014.
59. R. P. Verma and C. Hansch, “A Comparison between Two Polarizability Parameters in Chemical Biological Interactions,” *Bioorganic and Medicinal Chemistry* 13, no. 7 (2005): 2355–72. doi:10.1016/j.bmc.2005.01.051.
60. S. Shahaba and M. Sheikhi, “Antioxidant Properties of the Phorbol: A DFT Approach,” *Russian Journal of Physical Chemistry B* 14 (2020): 15–8. doi:10.1134/S199079312001045.
61. M. Raja, R. R. Muhamed, S. Muthu, and M. Suresh, “Synthesis, Spectroscopic (FT-IR, FT-Raman, NMR, UV-Visible), First Order Hyperpolarizability, NBO and Molecular Docking Study of (E)-1-(4-Bromobenzylidene)Semicarabzide,” *Journal of Molecular Structure* 1128 (2017): 481–92. doi:10.1016/j.molstruc.2016.09.017.
62. S. Sevvanthi, S. Muthu, and M. Raja, “Quantum Mechanical, Spectroscopic Studies and Molecular Docking Analysis on 5,5-Diphenylimidazolidine-2,4-Dione,” *Journal of Molecular Structure* 1149 (2017): 487–98. doi:10.1016/j.molstruc.2017.08.015.
63. C. Adant, M. Dupuis, and J. L. Bredas, “Ab Initio Study of the Nonlinear Optical Properties of Urea: Electron Correlation and Dispersion Effects,” *International Journal of Quantum Chemistry* 56, no. S29 (1995): 497–507. doi:10.1002/qua.560560853.
64. E. D. Glendening, A. E. Reed, J. E. Carpenter, and F. Weinhold, *NBO Version 3.1* (Madison: TCI, University of Wisconsin, 1998).
65. C. A. Lipinski, “Lead- and Drug-Like Compounds: The Rule-of-Five Revolution,” *Drug Discovery Today. Technologies* 1, no. 4 (2004): 337–41. doi:10.1016/j.ddtec.2004.11.007
66. A. K. Ghose, V. N. Viswanadhan, and J. J. Wendoloski, “A Knowledge-Based Approach in Designing Combinatorial or Medicinal Chemistry Libraries for Drug Discovery. 1. A Qualitative and Quantitative Characterization of Known Drug Databases,” *Journal of Combinatorial Chemistry* 1, no. 1 (1999): 55–68. doi:10.1021/cc9800071
67. C. Battilocchio, L. Guetzoyan, C. Cervetto, L. D. C. Mannelli, D. Frattaroli, I. R. Baxendale, G. Maura, A. Rossi, L. Sautebin, M. Biava, et al, “Flow Synthesis and Biological Studies of an Analgesic Adamantane Derivative That Inhibits P2X7-Evoked Glutamate Release,” *ACS Medicinal Chemistry Letters* 4, no. 8 (2013): 704–9. doi:10.1021/ml400079h
68. A. A. Spasov, T. V. Khamidova, L. I. Bugaeva, and I. S. Morozov, “Adamantane Derivatives: Pharmacological and Toxicological Properties (Review),” *Pharmaceutical Chemistry Journal* 34, no. 1 (2000): 1–9. doi:10.1007/BF02524549.
69. N. Fresno, R. Pérez-Fernández, C. Goicoechea, I. Alkorta, A. Fernández-Carvajal, R. de la Torre-Martínez, S. Quirce, A. Ferrer-Montiel, M. I. Martín, P. Goya, et al, “Adamantyl Analogues of Paracetamol as Potent Analgesic Drugs via Inhibition of TRPA1,” *PLoS One* 9, no. 12 (2014): e113841. doi:10.1371/journal.pone.0113841.
70. A. Lagunin, A. Stepanchikova, D. Filimonov, and V. Poroikov, “PASS: Prediction of Activity Spectra for Biologically Active Substances,” *Bioinformatics* 16, no. 8 (2000): 747–8. doi:10.1093/bioinformatics/16.8.747
71. O. Trott and A. J. Olson, “AutoDock Vina: Improving the Speed and Accuracy of Docking with a New Scoring Function, Efficient Optimization and Multithreading,” *Journal of Computational Chemistry* 31, no. 2 (2010): 455–61. doi:10.1002/jcc.21334.
72. B. Kramer, M. Rarey, and T. Lengauer, “Evaluation of the FlexX Incremental Construction Algorithm for Protein Ligand Docking,” *Proteins: Structure, Function, and Genetics* 37, no. 2 (1999): 228–41. doi:10.1002/(SICI)1097-0134(19991101)37:2 < 28::AID-PROT8 > 3.0.CO;2-8.
73. G. Venkatesh, Y. Sixto-Lopez, P. Vennila, Y. S. Mary, J. Correa-Basurto, Y. S. Mary, and A. Manikandan, “An Investigation on the Molecular Structure, Interaction with Metal Clusters, anti-Covid-19 Ability of 2-Deoxy-D-Glucose: DFT Calculations, MD and Docking Simulations,” *Journal of Molecular Structure* 1258 (2022): 132678. doi:10.1016/j.molstruc.2022.132678.
74. M. Smitha, Y. S. Mary, Y. S. Mary, G. Serdaroglu, P. Chowdhury, M. Rana, H. Umamahesvari, B. K. Sarojini, B. J. Mohan, and R. Pavithran, “Modeling the DFT Structural and Reactivity Studies of a Pyrimidine-6-Carboxylate Derivative with Reference to Its Wavefunction-Dependent, MD Simulations and Evaluation for Potential Antimicrobial Activity,” *Journal of Molecular Structure* 1237 (2021): 130397. doi:10.1016/j.molstruc.2021.130397.
75. Y. S. Mary, Y. S. Mary, O. Temiz-Arpaci, R. Yadav, and I. Celik, “DFT, Docking, MD Simulation, and Vibrational Spectra with SERS Analysis of a Benzoxazole Derivative: An anti-Cancerous Drug,” *Chemical Papers* 75, no. 8 (2021): 4269–84. doi:10.1007/s11696-021-01659-y.
76. Y. S. Mary, Y. S. Mary, A. S. Rad, R. Yadav, I. Celik, and S. Sarala, “Theoretical Investigation on the Reactive and Interaction Properties of Sorafenib-DFT, AIM, Spectroscopic and Hirshfeld Analysis, Docking and Dynamics Simulation,” *Journal of Molecular Liquids* 330 (2021): 115652. doi:10.1016/j.molliq.2021.115652.